AI–67–7

RADIATION EFFECTS ON SILVER AND ZINC BATTERY ELECTRODES

Final Report

April 1965 to October 1966

Prepared for

Jet Propulsion Laboratory

Under Contract No. 951109

ATOMICS INTERNATIONAL

A DIVISION OF NORTH AMERICAN AVIATION, INC.

This work was performed for the Jet Propulsion Laboratory, California Institute of Technology, pursuant to a subcontract issued under Prime Contract NAS7-100 between the California Institute of Technology and the United States of America Represented by the National Aeronautics and Space Administration.

167

RADIATION EFFECTS ON SILVER AND ZINC BATTERY ELECTRODES

Final Report
April 1965 to October 1966
Prepared for
Jet Propulsion Laboratory
Under Contract No. 951109

By

M. M. NICHOLSON
H. L. RECHT
G. R. ARGUE

ATOMICS INTERNATIONAL
A DIVISION OF NORTH AMERICAN AVIATION, INC.

JANUARY 30, 1967

CONTENTS

TABLES

FIGURES

I. ABSTRACT

Effects of gamma radiation on commercial secondary silver and zinc battery electrodes were investigated in experimental cells containing 40% potassium hydroxide electrolyte. Cells were examined at radiation doses of 7×10^7 to 9×10^8 rads (H_2O) for changes in discharge capacity, gas evolution, and loss of electrode material.

For the silver electrodes at 7×10^7 rads, average capacity changes associated with the irradiation process were -7% (±7%), +6% (±5%), and +1% (±9%) at 30, 60, and 90% states of charge, respectively. Pressure increases up to 0.8 atm, due primarily to the radiolytic evolution of hydrogen and oxygen, were observed at the same dose level in silver test cells with cadmium counter electrodes. Material losses from unsupported silver-silver oxide electrodes in flooded cells averaged 1.4% of the silver electrode weight.

Zinc electrodes were studied less extensively because of the inherent limitations on their electrochemical reproducibility. An apparent increase in zinc discharge capacity during irradiation probably was caused by changes in the physical characteristics of the cellophane separator. Hydrogen evolution also occurred in zinc cells. Solid material losses were not directly measurable in the closely-packed starved-electrolyte design that was necessary to obtain quantitative capacity data.

Of all the radiation effects investigated, only gas evolution appears to present a special design requirement for silver-zinc batteries in space applications.

II. INTRODUCTION

Batteries in space vehicles may be exposed to cosmic rays and to the more intense radiation field of the Van Allen belt. In nuclear space systems, still higher radiation doses are generated internally. For example, both nickel-cadmium and silver-zinc batteries in the 43-day SNAP-10A mission received a radiation dose of 10^6 rads (H_2O). An earlier program demonstrated that this dose level is at the threshold for radiation damage in the nickel-cadmium system.[1] The present program was undertaken to establish comparable information for the silver-zinc system.

Detailed results of this work for the period extending from April 1965 to July 1966 have been presented in a series of interim reports.[2-6] This final report on the silver-zinc study contains a detailed description of work performed since the fifth interim report and a summary of procedures and results for the entire program.

III. EXPERIMENTAL

A. METHOD OF INVESTIGATION

Radiation doses of magnitudes that may be encountered by batteries in space environments were simulated with shorter exposures in high-intensity Co^{60} gamma radiation sources. The behavior of commercial battery electrodes in 40% potassium hydroxide electrolyte was examined in experimental cells that were designed to permit the measurement of discharge capacity changes, gas evolution, and material losses associated with the irradiation process. Essential features of the equipment and experimental procedures are reviewed in Sections B through E below. Further details are given in the interim reports.[2-6]

B. CELLS AND ELECTRODES

Outer containers for the experimental cells were constructed of stainless steel, with pressure-tight O-ring seals and insulated feed-through connections for the electrode leads. In several runs, miniature strain-gage transducers with ranges of $\pm$12.5 psig or $\pm$25 psig were mounted in the stainless steel lids for the recording of pressure. A photograph of the cell assembly shown in Figure 1.

The electrodes and electrolyte were place in alkali-resistant cell liners inside the steel cases. Most of the liners were made of polystyrene, with fritted quartz separators, as illustrated in Figure 2. An all-quartz cell of similar design was used in an early stage of the work.[2]

In a preliminary investigation of silver-zinc cells, the zinc electrode disintegrated after several charge-discharge cycles.[2] The

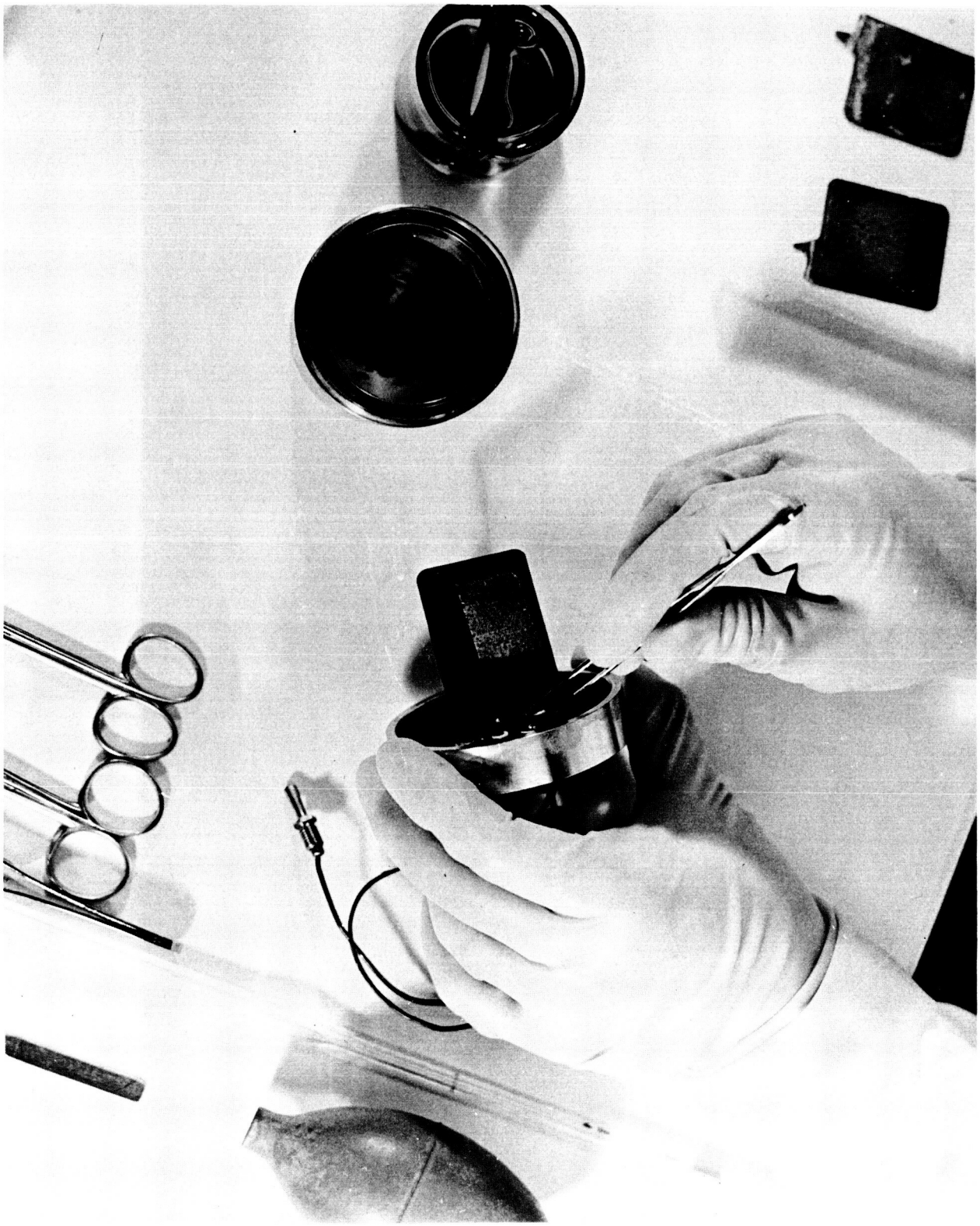

FIGURE 1. ASSEMBLY OF STAINLESS STEEL-CASED CELL FOR SILVER ELECTRODE STUDIES

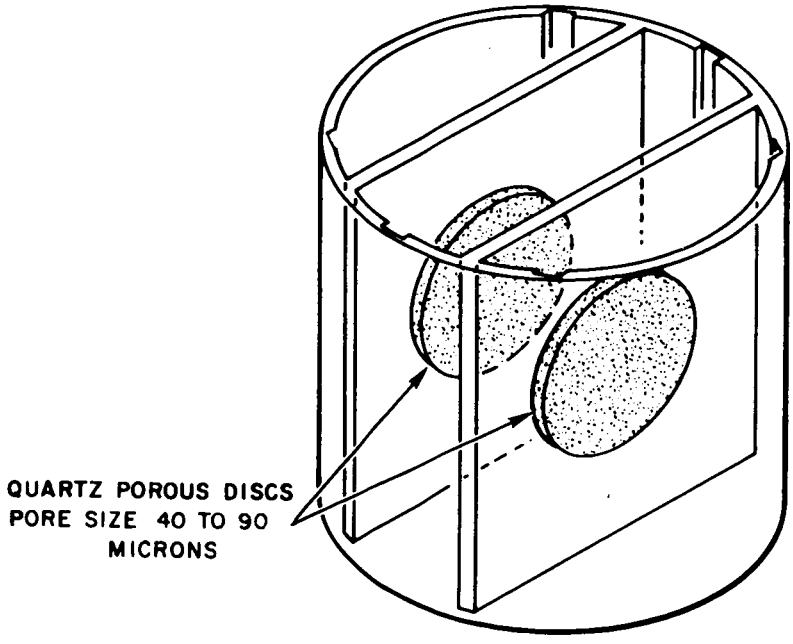

FIGURE 2. POLYSTYRENE CELL LINER

more quantitative studies were therefore concentrated initially on silver electrode behavior in silver-cadmium cells. The silver test electrodes were sections cut from Yardney Electric Corporation 0.8 amp-hr electrodes. Most of the sections used had a weight of 1.5 g and a nominal capacity of 0.4 amp-hr. The silver electrode was inserted in the central compartment of the liner shown in Figure 2. Two parallel-connected cadmium counter electrodes, each with a nominal capacity of 0.5 amp-hr, were placed in the outer compartments to give a uniform current density distribution on the test specimen. The silver electrode was thus made capacity-limiting. Initially, the cadmium electrodes were those removed from Eveready N-75 nickel-cadmium cells and trimmed to fit the polystyrene liners. It was later found more convenient to use Eveready R-2 cadmium plates, which were of similar construction but required no trimming.[5]

Mercury-mercuric oxide reference electrodes of the design illustrated in Figure 3 were used in the cells occasionally to characterize individual electrode behavior and to minimize the influence of ohmic drop in the automatic current control system.[5]

The performance of zinc electrodes in flooded cells was unsatisfactory, due to growth of dendrites and excessive material loss on cycling.[2] The experimental development of starved-electrolyte zinc cells with cellophane separators that was begun during the fifth report period was continued in the more recent work reported here. A diagram of such a cell is shown in Figure 4. This assembly was placed inside the same kind of stainless steel case that was used for the silver electrode studies.

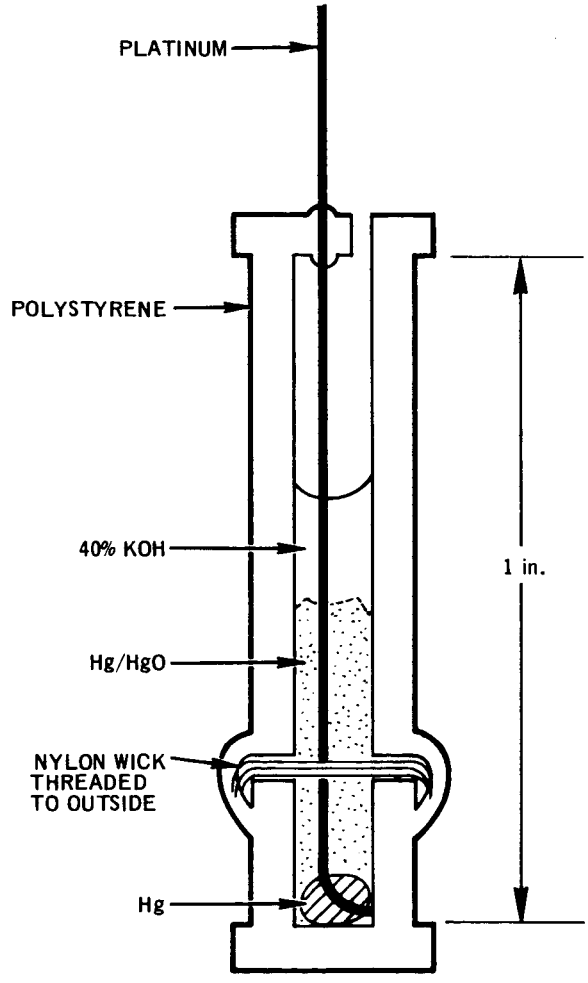

11-16-66 UNC 00-25202

FIGURE 3. REFERENCE ELECTRODE

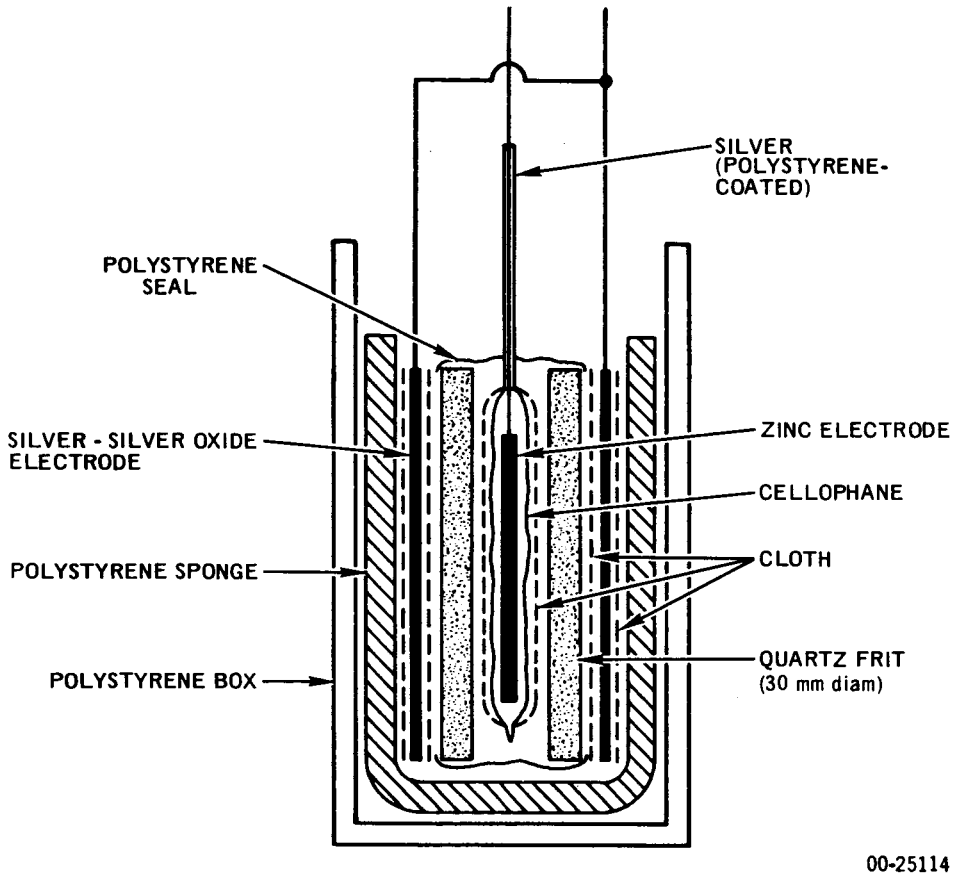

FIGURE 4. STARVED-ELECTROLYTE SILVER-ZINC CELL

The zinc electrodes (except in Run ZG-7)[6] were sections of zinc plates from Yardney Electric Corporation. These plates had a relatively heavy layer of porous zinc attached to each side of a copper foil backing. Previously charged silver plates with excess capacity served as counter electrodes in the zinc studies.

C. ELECTRICAL CIRCUITS

The instrumentation was designed to perform two principle functions: (1) automatic shallow cycling in four phases, each of 15 minutes duration, and (2) automatic complete charge-discharge cycling at constant current for the measurement of capacity. In each operation, the voltage between the test electrode and the reference or counter electrode was recorded as a function of time.

The elements of the two automatic systems are indicated schematically in Figures 5 and 6. The shallow cycling regime provided the sequence charge-open circuit-discharge-open circuit, with a cycle depth of 5%. The capacity-measuring system operated at a constant charging or discharging current until the total cell voltage or the voltage of the test electrode versus the reference electrode reached a preset limit. The monitored voltage was then maintained at the upper or lower limit by intermittent application of the current in response to an electronic control system. Finally, automatic current reversal occurred at the end of several hours. The capacity-measuring circuit, modified to permit control, as well as recording, against a high-impedance reference electrode, is diagrammed in Figure 7. Details of this modification are discussed in the Fourth Interim Report.[5]

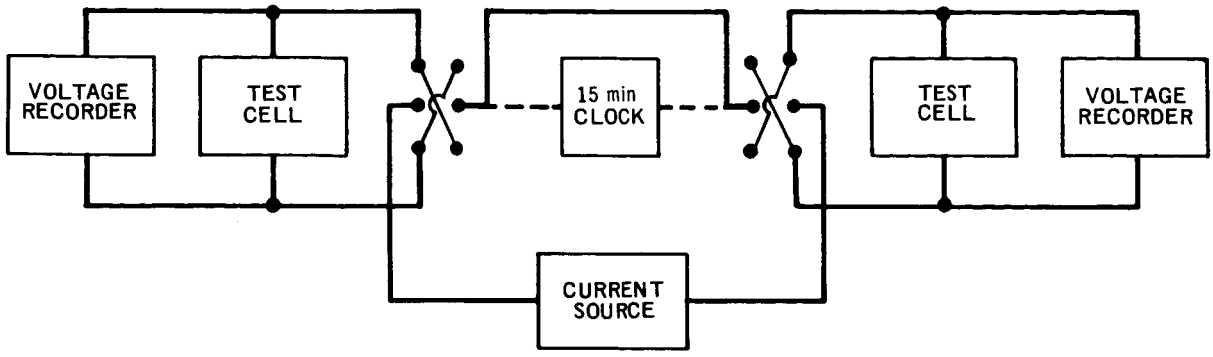

10-16-66 UNC 00-25200

FIGURE 5. SCHEMATIC DIAGRAM OF CYCLING CIRCUIT

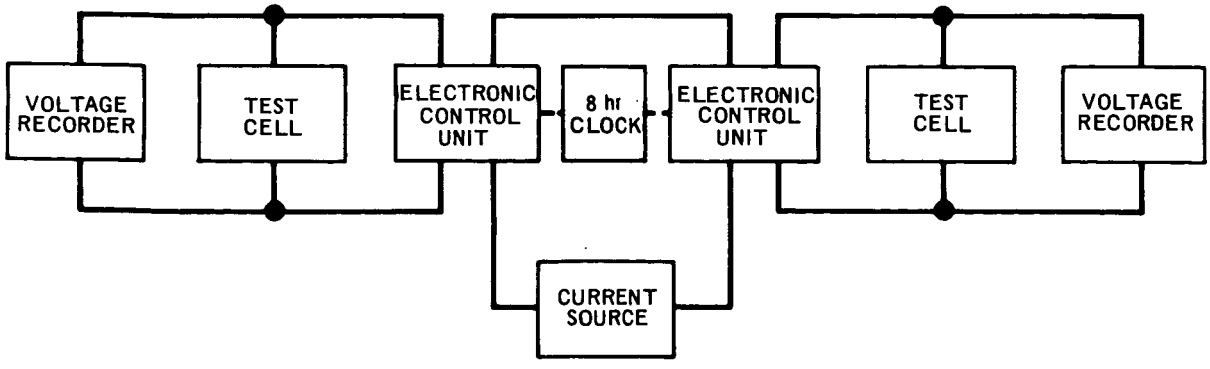

10-16-66 UNC 00-25201

FIGURE 6. SCHEMATIC DIAGRAM OF CAPACITY MEASURING CIRCUIT

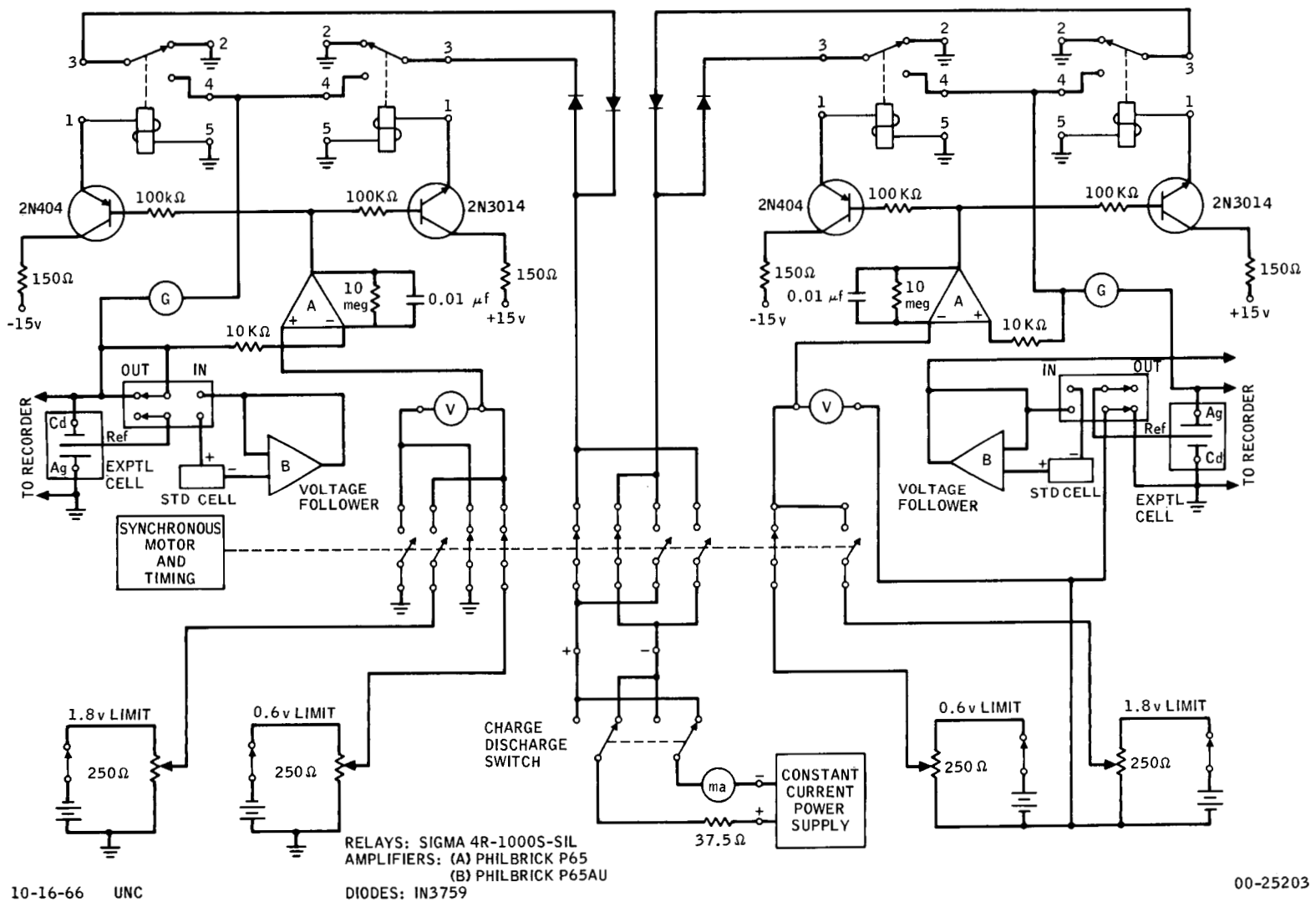

FIGURE 7. MODIFIED CAPACITY MEASURING CIRCUIT

D. GAMMA RADIATION SOURCES

Most of the irradiation experiments were performed in the 10^6 rad/hr Co^{60} gamma source at the North American Aviation Science Center. The measured temperature of cells equilibrated in the radiation zone of this source was 40 to 45°C.

Toward the end of the program, the new NAA Gamma Facility at Atomics International became available. In this larger source, the dose rate could be varied from a maximum value of 2×10^7 rads/hr by appropriate spacing of the Co^{60} rods. The cell temperature in the larger source was maintained at 47° or lower by forced air convection.

E. PROCEDURES

1. Silver Electrode Studies

The silver-cadmium cells were prepared in duplicate for each run; one cell was irradiated, while the other served as a control. After charging to the initial full capacity of the silver electrode, as determined by the voltage rise at the onset of oxygen evolution, the cells were preconditioned by cycling for 24 hrs at the desired state of charge ($Q \rightleftharpoons Q + \Delta Q$). Q was 30, 60 or 90% of full charge, and ΔQ was 5%. After cycling, the pre-irradiation capacity was determined more precisely in several complete charge-discharge cycles. Both cells were cycled again at $Q \rightleftharpoons Q + \Delta Q$ during the irradiation stage. Following this step, the post-irradiation capacities were measured, the gas atmospheres were analyzed, and the residual solids in each cell compartment were removed for analysis.* The complete procedure for the silver electrodes is diagrammed in Figure 8.

Certain steps included in this chart were developed after the second report period, in efforts to improve the precision of the capacity

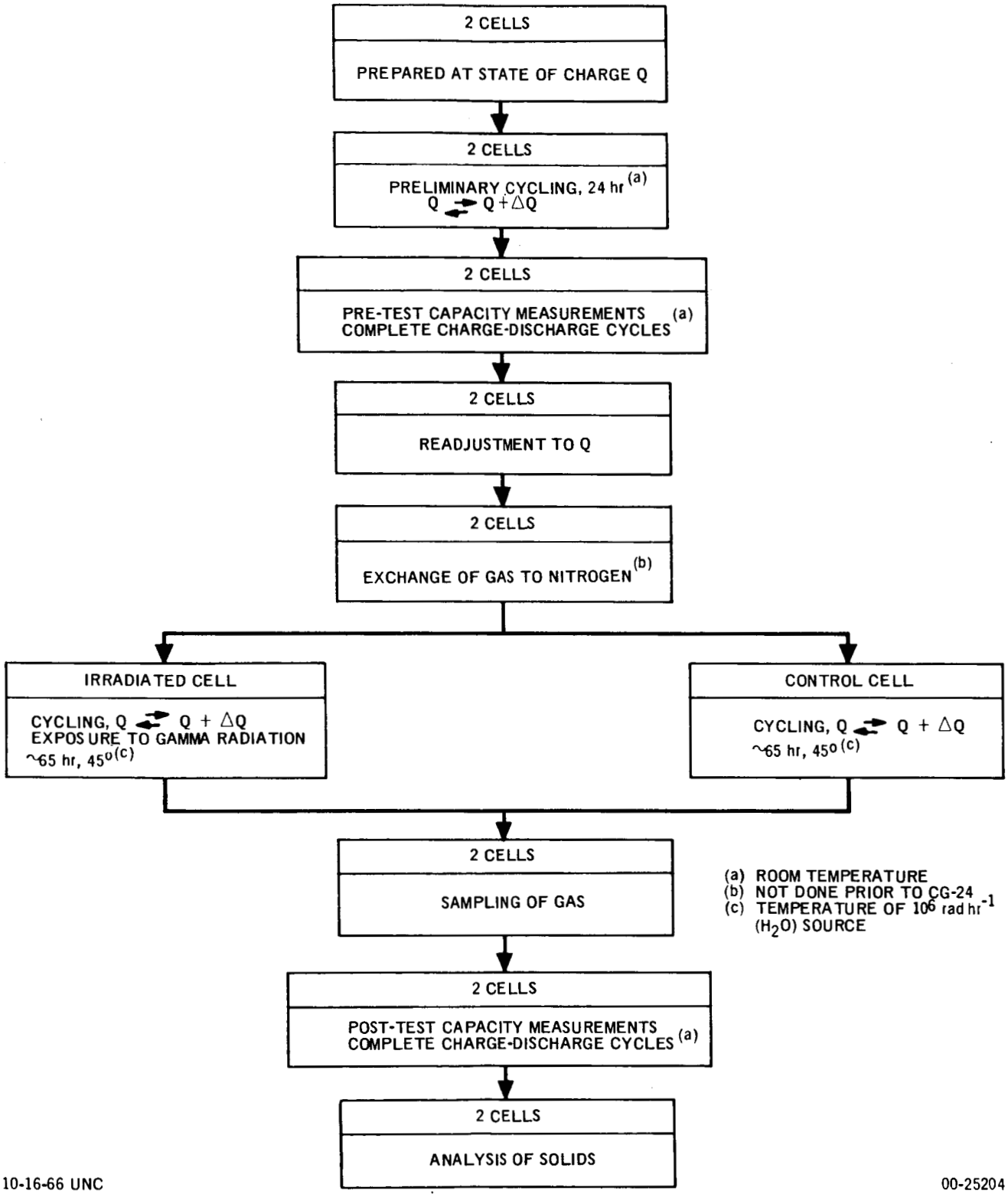

FIGURE 8. EXPERIMENTAL PROCEDURE FOR SILVER ELECTRODES

and gas evolution data. The discharge current density in the capacity measurements was kept at a standard value of 7.2 ma/cm^2. Pre-irradiation cycling was done at the source temperature rather than at room temperature. The sealed cells were examined for leaks with a mass spectrometer leak detector, and the cell atmosphere was replaced with nitrogen immediately before the irradiation stage to simplify the interpretation of gas composition data.

2. Zinc Electrode Studies

Extensive preconditioning was less effective in stabilization of the zinc electrodes because their behavior appeared to be very dependent on the maintenance of an unbroken separator envelope. Although the electrolyte was presaturated with zinc oxide to minimize the loss of electrode material by dissolution in the discharged stage, the possibility remained, in flooded cells, for the continuous buildup of zinc in the charging stage. This problem was mitigated by the starved-electrolyte design, but the measured capacity was then very probably influenced by the characteristics of the separator material and the cell geometry.

The zinc capacity measurements could not be made with the automatic voltage-limited system that was used for the silver electrodes because the cellophane envelope would be broken by the pressure of hydrogen accumulating during lengthy overcharges. By increasing the current density at the zinc electrode from 7.2 to 14 ma/cm^2, three discharges could be obtained in one day with manual switching. This higher current density was applied in Runs ZG-11, ZG-12, and ZG-13, for which results are given in this report.

IV. RESULTS AND DISCUSSION

Recent results on silver and zinc electrodes that were not included in earlier reports are presented in Sections A and B below. Cumulative results on silver for the entire program are summarized and discussed in Section C.

A. SILVER ELECTRODES AT HIGH RADIATION DOSES

Two irradiation runs were made on silver electrodes at 90% state of charge in the high-intensity gamma source at Atomics International. Heating rates at these dose rates were substantially greater than those encountered in the smaller source that was used in the earlier parts of the program. To establish cooling requirements, the curves in Figure 9 were obtained by means of a thermocouple placed inside one of the closed stainless steel cells containing a plastic liner and the usual volume of electrolyte. At the maximum dose rate of 2×10^7 rads (H_2O)/hr, without forced convection, the temperature inside the cell approached 100°C at the end of 3.5 hrs. Under forced convection provided by a fan, the temperature at the maximum rate was stabilized at 47°C, as shown in parts (a) and (b) of this figure. At one-half the maximum dose rate, which was obtained by the use of 6 cobalt rods instead of 12, the steady-state temperature was 37° with the fan. Temperatures of 40 to 45° had been measured in the smaller gamma source without forced convection.

Detailed conditions for the two silver electrode runs are given in Table I. In Run CG-35, the total dose was twice that used in the earlier runs; in CG-36, it was 13 times the original value. With the

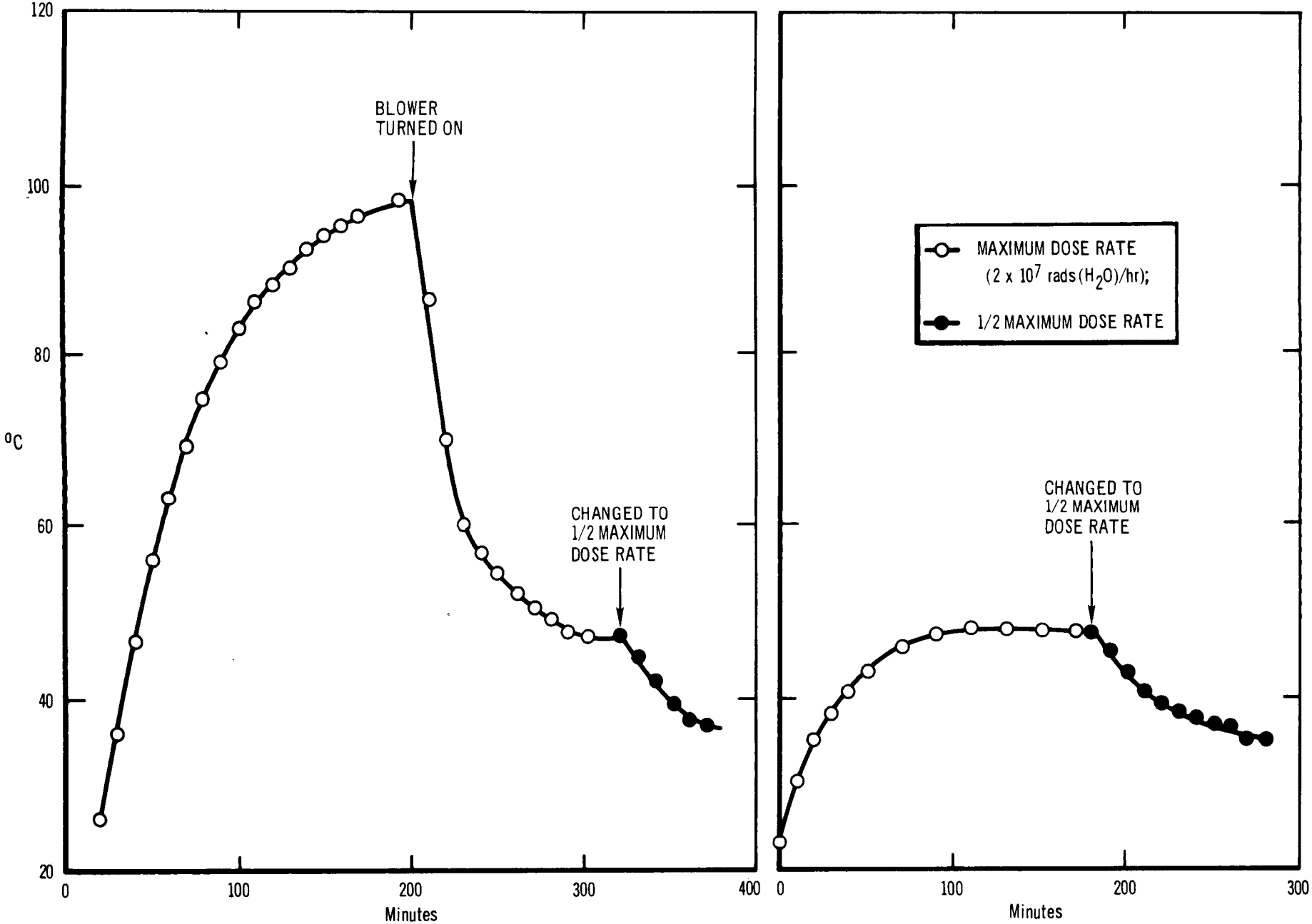

AI-67-7
16

(a) IRRADIATION BEGUN WITHOUT FORCED CONVECTION

(c) IRRADIATION WITH FORCED CONVECTION

11-17-66 UNC

00-25199

FIGURE 9. TIME-DEPENDENCE OF CELL TEMPERATURE IN AI GAMMA SOURCE

TABLE I. CONDITIONS FOR SILVER ELECTRODE RUNS[a]

Run	Irradiation: Dose Rate (rads/hr)	Irradiation: Total Dose (rads(H_2O))	Initial State of Charge (%)	Silver Electrode: Weight[b] (g)	Silver Electrode: Area[c] (cm^2)	Capacity Measurements: Total Current (ma)	Capacity Measurements: Current Density (ma/cm^2)	Irradiation Cycling Current[a] (ma)
CG-35			90					
Irradiated Cell	11×10^7	1.5×10^8		1.46	13.6	99	7.3	83
Control Cell	0	0		1.43	13.8	99	7.2	81
CG-36			90					
Irradiated Cell	2×10^7	9×10^8		1.40	13.8	101	7.3	88
Control Cell	0	0		1.39	14.0	101	7.3	85

[a]Preconditioned 90 $\rightleftharpoons$ 95%, 24 hr, 45°

[b]Corrected for weight of leads, but including embedded silver grid

[c]Total projected area, including both sides

[d]Selected for 5% cycle depth in 15 minutes

exception of dose rate and cell temperature, the other conditions in these runs were essentially those of the previous work. Discharge capacities of the silver electrodes are given in Table II. The capacity increases observed in the irradiated cells are within the range of those in earlier runs at the 90% charge level. The zero net capacity charge in Run CG-35 is not directly comparable to earlier data because of a temperature error in the control cell. The net charge of -6% in Run CG-36 lies within the statistical average of changes for 90% runs at 7×10^7 rads (Section C). Hence, it appears that gamma radiation doses as high as 10^9 rads (H_2O) have little, if any, effect on the silver electrode capacity at this charge level.

Gas pressures and compositions from the high-dose silver runs are listed in Table III, and a pressure vs time recording for Run CG-36 is reproduced in Figure 10. This curve has the same general shape as those recorded at the lower dose rate of the smaller source, although the total pressure increase of 0.6 atm was not quite as large. Radiation damage to the rubber O-ring or other sealing materials at the high dose condition may account for the relatively small pressure increase observed in that case. Significant quantities of hydrogen were produced by radiolysis, as in earlier runs with silver-cadmium cells.*

The weights of residual solids in the silver electrode compartments (Table IV) did not increase with the high radiation doses. Further investigation would be required to explain this result, which is

*Hydrogen evolution is discussed further in Section IV.B.2.

TABLE II. SILVER ELECTRODE CAPACITY IN IRRADIATION RUNS

Run	Initial State of Charge (%)	Cycle	Irradiated Cell				Control Cell			
			Pre-Test Capacity		Post-Test Capacity		Pre-Test Capacity		Post-Test Capacity	
			(amp-hr)	Δ[a]	(amp-hr)	Δ[a]	(amp-hr)	Δ[a]	(amp-hr)	Δ[a]
CG-35[b]	90	1	0.396	-0.015	0.468	+0.005	0.399	-0.008	0.464	+0.005
		2	0.423	+0.012	0.461	-0.002	0.416	+0.009	0.452	-0.007
		Average	0.411	±0.013	0.463	±0.003	0.407	±0.009	0.459	±0.006
		Change		+13% (±4%)				+13% (±4%)[c]		
CG-36[d]	90	1	0.442	+0.001	0.467	+0.004	0.416	-0.008	0.474	+0.005
		2	0.440	-0.001	0.458	-0.005	0.430	+0.006	0.462	-0.007
		Average	0.441	±0.001	0.463	±0.005	0.424	±0.007	0.469	±0.006
		Change		+5% (±1%)				+11% (±3%)		

[a] Deviation from average

[b] Total dose 1.5×10^8 rads (H_2O)

[c] Temperature was 47° in control cell, 37° in irradiated cell

[d] Total dose 9×10^8 rads (H_2O)

TABLE III. ANALYSES[a] OF GASES IN SILVER-CADMIUM CELLS AFTER IRRADIATION STAGE

Run	Initial State of Charge[b] (%)	Gas Volume (ml)	Total Pressure (mm Hg)	Volume Percent[c]						
				O_2	N_2	Ar	H_2O	CH_4	CO_2	H_2
CG-35	90									
Irradiated Cell		47	777	0.18	87.00	0.04	2.89	0.11	0.13	9.76
Control Cell[d]		--	--	--	--	--	--	--	--	--
CG-36	90									
Irradiated Cell		43	928	0.23	59.60	0.13	0.41	0.43	0.12	39.10
Control Cell		49	760	10.51	85.77	0.22	3.67	0	0.13	0

[a] Mass spectroscopy

[b] Silver electrode

[c] Cells were flushed with nitrogen immediately before the irradiation stage

[d] Faulty sampling

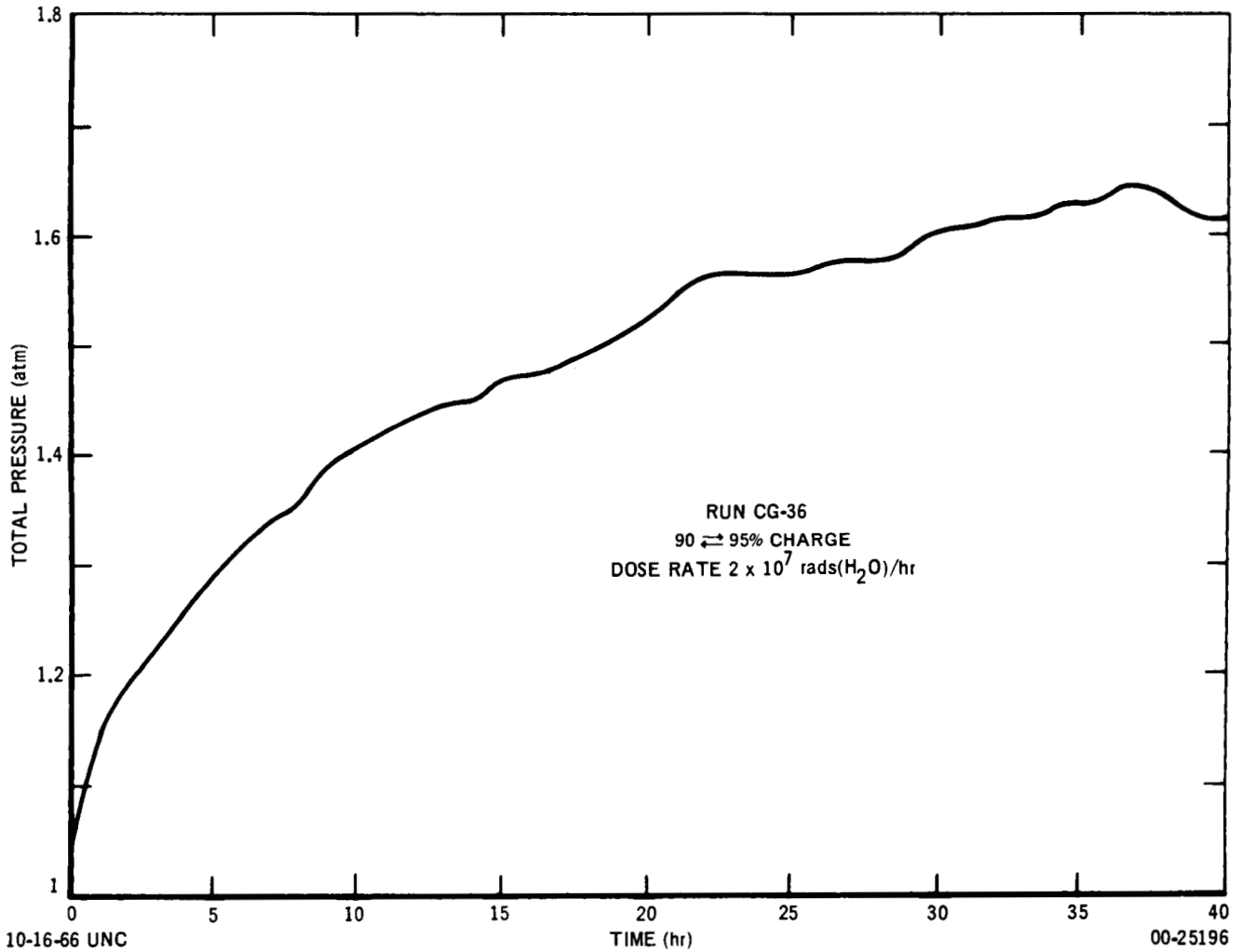

FIGURE 10. PRESSURE CHANGE AT 90% STATE OF CHARGE AND MAXIMUM DOSE RATE

TABLE IV. ANALYSES OF SOLIDS RECOVERED FROM SILVER ELECTRODE COMPARTMENT

Run	Initial State of Charge (%)	Total Wt (mg)	Wt % SiO_2 [a]	Net Wt (mg)	Identified [b]	Wt Cd/Wt Ag [c]
CG-35	90					
Irradiated Cell		8.4	3	8.1	Ag	0.023
Control Cell		1.7	---[d]	~1.7	Ag, $Cd(OH)_2$	---[d]
CG-36	90					
Irradiated Cell		14.6	9	14.2	Ag	0.016
Control Cell		3.9	---[d]	~4	Ag, $Cd(OH)_2$	0.29

[a] Emission spectroscopy

[b] X-ray diffraction

[c] X-ray fluorescence

[d] Insufficient sample

based on comparisons with only two high-dose runs. A summary of silver solids data for the entire program is included in Section C.

The weights and compositions of cadmium compartment residues (Table V) were consistent with those found in earlier runs with the R-2 cadmium electrodes. This result was anticipated, since no significant material loss from these electrodes has been associated with the irradiation process.

B. RADIATION EFFECTS ON ZINC ELECTRODES

Experimental conditions for the zinc electrode runs, including certain details of the cell construction, are listed in Table VI. In preliminary experiments, the Permion 600 cellophane, a pre-irradiated material, was found to be much more resistant to gamma rays than the nonirradiated battery grade Pudo 193. Permion envelopes were therefore used in the zinc irradiation runs. The Viskon padding, a nonwoven cellulose fabric, was also severely attacked when irradiated in the alkaline solution. Its destruction prevented the measurement of post-test capacity in the irradiated cell of Run ZG-12. By replacing the Viskon with a separator cloth from the R-2 cells, both pre- and post-irradiation data were obtained in Run ZG-13.

The zinc electrode capacities are given in Table VII. Typical charging and discharging curves for zinc are shown in Figure 11. When cycled from an initial 90% state of charge the zinc electrode showed an <u>apparent</u> net capacity gain of 41% due to irradiation. This change probably reflects increased permeability of the envelope material, rather than an intrinsic change in the electrode system.

Table VIII contains gas evolution data for the zinc cells. Hydrogen

TABLE V. ANALYSES OF SOLIDS RECOVERED FROM CADMIUM ELECTRODE COMPARTMENTS

Run	Initial State of Charge (%)	Total Wt (mg)	Wt % SiO_2 [a]	Net Wt (mg)	Identified [b]	Wt Cd/Wt Ag [c]
CG-35						
Irradiation Cell		3.2	---[d]	~3	Ag, $Cd(OH)_2$	1.0
Control Cell		5.2	5	4.9	Ag, $Cd(OH)_2$	0.88
CG-36						
Irradiated Cell		8.8	4	8.5	Ag, $Cd(OH)_2$	1.12
Control Cell		5.8	---[d]	~6	Ag, $Cd(OH)_2$	1.80

[a] Emission spectroscopy

[b] X-ray diffraction

[c] X-ray fluorescence

[d] Insufficient sample

TABLE VI. CONDITIONS FOR ZINC ELECTRODE RUNS

Run	Cell Construction[a]				Irradiation Conditions			Observations
	Cello-phane	Inner Padding	Outer Padding	Wt Zinc (g)	Cycling[b]	Dose Rate (rads/hr)	Total Dose (rads(H_2O))	
ZG-11	Pudo 193	Viskon	Viskon	0.36	90 $\rightleftharpoons$ 95% 2 hr, 25°	0	0	Electrode appeared in good condition after 1 week, 11 discharges
ZG-12	Permion 600	Viskon	Viskon	0.42[c] 0.42[d]	None	1×10^7	3×10^8	Viskon was destroyed by radiation; post-irradiation capacity not measurable
ZG-13	Permion 600	Cloth[e]	Poly-styrene sponge[f]	0.40[c] 0.42[d]	90 $\rightleftharpoons$ 95% 28 hr, 37°	1×10^7	3×10^8	Cells remained intact

[a]Starved electrolyte design (Figure 4)

[b]No cycling before the irradiation stage

[c]Irradiated cell

[d]Control cell

[e]Removed from Eveready R-2 cell

[f]Thickness ~3 mm

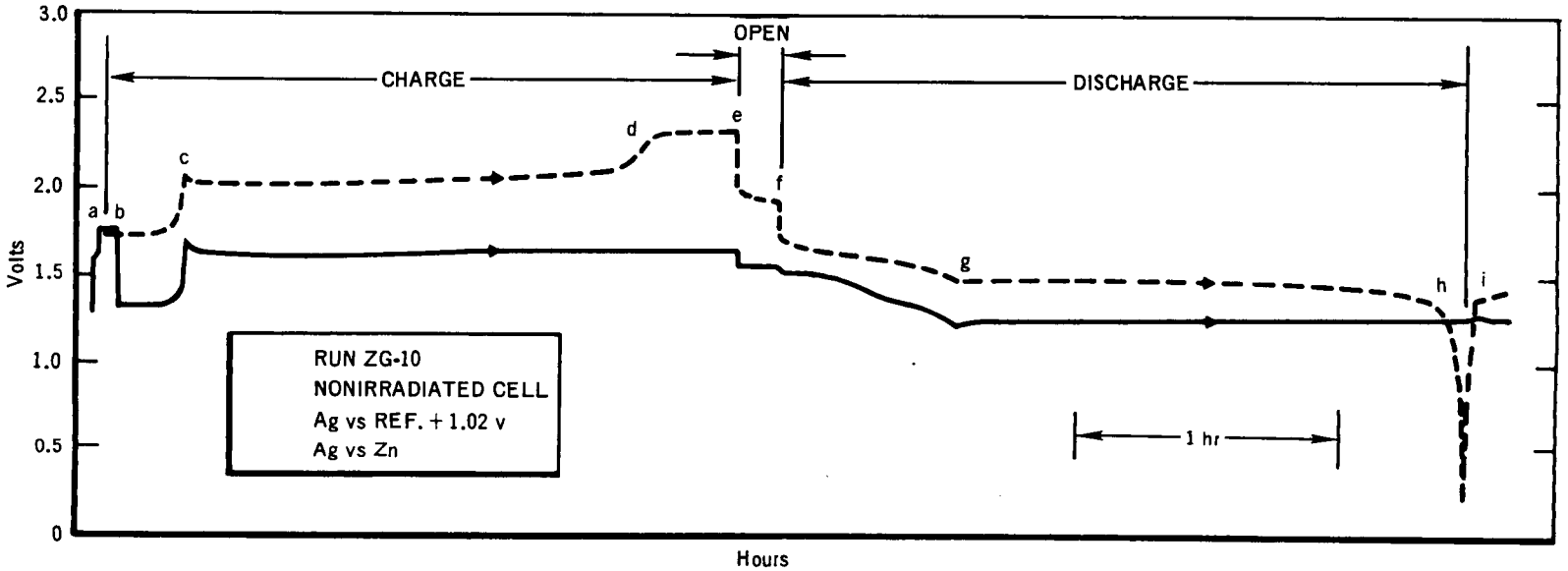

(a) BEGINNING OF CHARGE AT 36 ma
(b) REFERENCE SYSTEM SWITCHED IN
(c) Ag_2O/AgO TRANSITION
(d) Zn OVERCHARGE; EVOLUTION OF H_2
(e) OPEN CIRCUIT
(f) BEGINNING OF DISCHARGE AT 36 ma
(g) AgO/Ag_2O TRANSITION
(h) END OF Zn DISCHARGE
(i) OPEN CIRCUIT

10-17-66 UNC

00-25115A

FIGURE 11. POTENTIAL-TIME CURVES FOR SILVER-ZINC CELL[6]

TABLE VII. ZINC ELECTRODE CAPACITY

Run	Initial State of Charge (%)	Cycle	Irradiated Cell				Control Cell			
			Pre-Test Capacity		Post-Test Capacity		Pre-Test Capacity		Post Test Capacity	
			(amp-hr)	Δ[a]	(amp-hr)	Δ[a]	(amp-hr)	Δ[a]	(amp-hr)	Δ[a]
ZG-11	90	1	---[b]	---	---	---	0.045[c]	---	0.172	+0.038
		2					0.170	-0.013	0.164	+0.030
		3					0.196	+0.013	0.149	+0.015
		4							0.139	+0.005
		5							0.120	-0.014
		6							0.103	-0.031
		7							0.114	-0.020
		8							0.109	-0.025
		Average					0.183	±0.013	0.134[d]	±0.022
ZG-12[e]	100[f]	1	0.104	-0.002	---[g]	---	0.064	+0.002	0.045	-0.001
		2	0.109	+0.003			0.061	-0.001	0.046	0.000
		Average	0.106	±0.003			0.062	±0.002	0.046	±0.000
ZG-13[e]	90	1	0.064	-0.002	0.085	-0.005	0.074	-0.001	0.068	-0.003
		2	0.069	+0.003	0.094	+0.004	0.077	+0.002	0.074	+0.003
		Average	0.066	±0.002	0.090	±0.004	0.075	±0.002	0.071	±0.003
		Change	+36% (±9%)					-5% (±7%)		

[a] Deviation from average

[b] No irradiation

[c] Omitted from average

[d] Post-cycling capacity measurements extended over 1 week

[e] Total dose 3×10^8 rads (H_2O)

[f] Not cycled

[g] Viskon separator destroyed by radiation; post-test capacity not measurable

TABLE VIII. ANALYSES[a] OF GASES IN SILVER-ZINC CELLS AFTER IRRADIATION STAGE

Run	Initial State of Charge[b] (%)	Gas Volume (ml)	Total Pressure (mm Hg)	Volume Percent						
				O_2	N_2	Ar	H_2O	CH_4	CO_2	H_2
ZG-12	90									
Irradiated Cell		--	--	0.04	59.1	0.02	1.26	0	0	39.6
Control Cell[c]		--	--	--	--	--	--	--	--	--
ZG-13	90									
Irradiated Cell		129	756	0.05	91.8	0.05	2.08	0.10	0.12	5.88
Control Cell		128	737	0.94	94.0	0.23	3.73	0.12	0.21	0.77

[a]Mass spectroscopy

[b]Zinc electrode

[c]Faulty sampling

appeared as a major product of radiolysis, as in the silver-cadmium runs. Its formation in such systems is believed to accompany the consumption of hydroxyl radicals by the active metal electrode.[3] The envelope in Run ZG-13 may then have been penetrated to some extent by both OH· and H_2. The radiolytic decomposition of organic materials may provide another source of hydrogen. This kind of reaction probably accounts for a major portion of the hydrogen in Run ZG-12 and a minor portion in Run ZG-13.

Further study by modified experimental approaches would be required to evaluate radiation effects on zinc electrode systems more quantitatively. This is especially true of secondary electrodes, for which the interfacial processes tend to be obscured by transport phenomena.

C. SUMMARY OF RADIATION EFFECTS ON SILVER ELECTRODES

Gamma radiation effects on silver electrodes are summarized in this section for the entire program. Of the three phenomena that were investigated rather extensively, only one, the evolution of gases, was found to have a potential major influence on battery performance at radiation doses in the 10^8 to 10^9 rad range. The other variables examined, which were discharge capacity and material loss, showed only small radiation effects that should not necessitate any major design changes in silver-zinc batteries for presently-scheduled space missions.

1. Discharge Capacity

Representative charging and discharging curves for silver electrodes are shown in Figure 12. Discharge capacity changes at 90, 60, and 30% states of charge are summarized in the three parts of Table IX and represented graphically in Figure 13. In most runs, the capacity changes

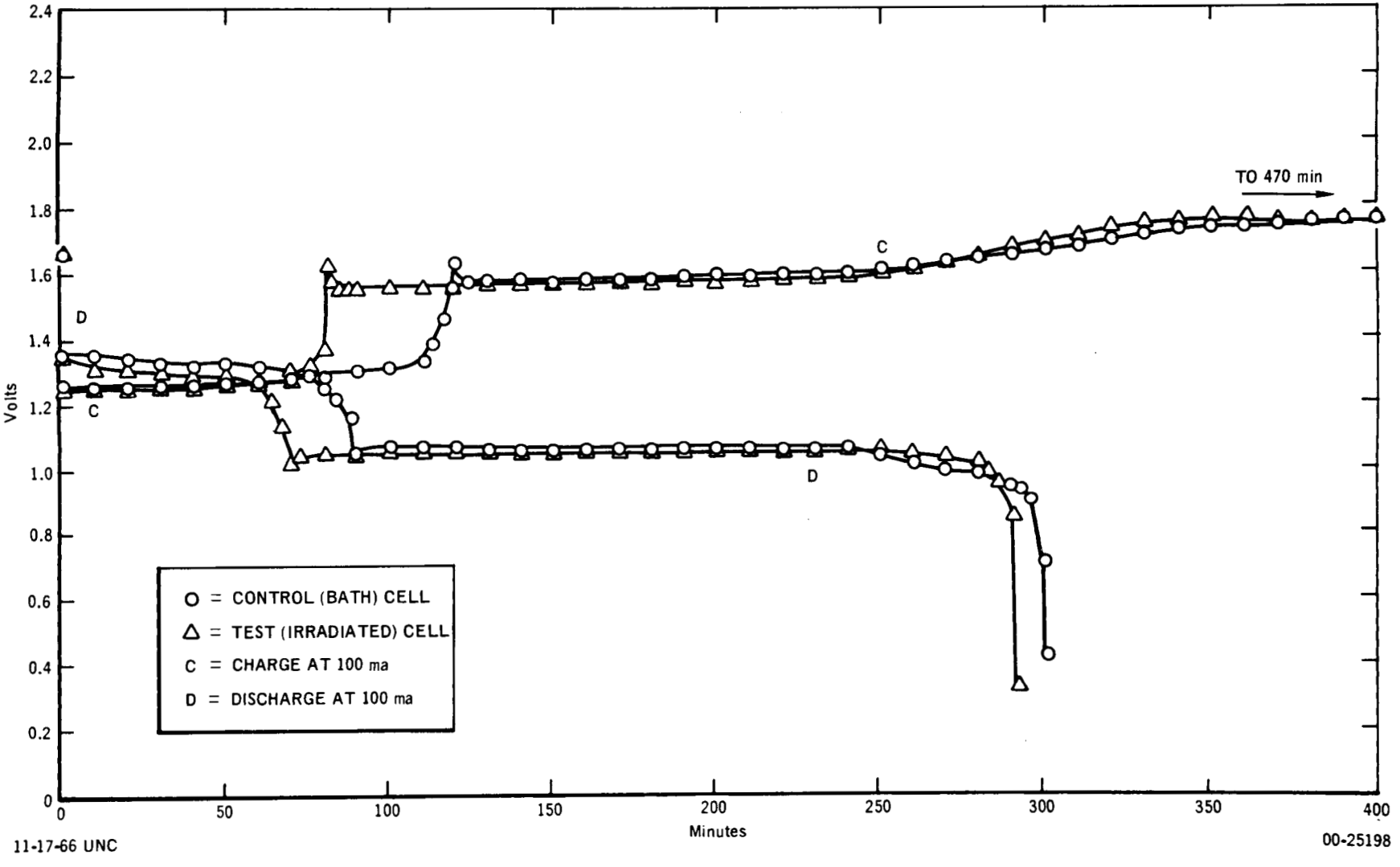

FIGURE 12. CHARGE AND DISCHARGE CURVES FOR Ag-Cd CELLS PRIOR TO IRRADIATION TESTING (DATA FOR RUN #CG-17)

TABLE IX. CHANGE IN SILVER ELECTRODE CAPACITY DURING IRRADIATION STAGE

(A) Runs at 90% Initial State of Charge

Run	Report[a]	Capacity Change (%)		
		Irradiated Cell[b]	Control Cell	Net Change[c]
CG-9	II	-16 (±1)[d]	-7 (±3)[d]	-9[d]
CG-10	II	+5 (±3)	+4 (±3)	+1
CG-11	II	+5 (±2)	+15 (±14)	-10
CG-15	II	+4 (±4)	+2 (±9)	+2
CG-16	II	+15 (±6)	0 (±6)	+15
CG-22	III	+11 (±1)	---	---
CG-23	III	+15 (±3)	+12 (±2)	+3
CG-24	IV	+21 (±2)	+15 (±2)	+6
CG-25	IV	+10 (±3)	+17 (±3)	-7
	Average	+11 (±3)	+9 (±6)	+1 (±9)
CG-35[e]	Final	+13 (±4)	+13 (±4)[f]	---
CG-36[g]	Final	+5 (±1)	+11 (±3)	-6

[a] Detailed data are given in the indicated report on this program

[b] Total dose 7×10^7 rads (H_2O) unless noted

[c] Change in irradiated cell minus change in control cell

[d] Omitted from average (only one capacity measurement)

[e] 1.5×10^8 rads (H_2O)

[f] Control cell temperature 10° too high

[g] 9×10^8 rads (H_2O)

TABLE IX. (Continued)

(B) Runs at 60% Initial State of Charge

Run	Report[a]	Capacity Change (%)		
		Irradiated Cell[b]	Control Cell	Net Change[c]
CG-12	II	-6 (±7)	-2 (±4)	-3
CG-13	II	0 (±4)	-6 (±7)	+6
CG-14	II	+10 (±4)	-1 (±4)	+11
CG-17	II	0 (±1)	-11 (±2)	+11
CG-18	II	---[d]	-22 (±6)	---
CG-26	IV	+3 (±4)	+7 (±4)	-4
CG-27	IV	+17 (±6)	+11 (±3)	+6
CG-29	IV	---[e]	+4 (±3)	---
CG-30	IV	+15 (±3)	+8 (±3)	+7
CG-31	V	+18 (±1)	+6 (±3)	+12
	Average	+7 (±4)	-1 (±4)	+6 (±5)

[a] Detailed data are given in the indicated report on this program

[b] Total dose 7 x 10^7 rads (H_2O)

[c] Change in irradiated cell minus change in control cell

[d] Electrolyte partially spilled

[e] Cycling current off control

TABLE IX. (Continued)

(C) Runs at 30% Initial State of Charge

Run	Report[a]	Capacity Change (%)		
		Irradiated Cell[b]	Control Cell	Net Change
CG-19	II	-19 (±5)	-22 (±2)	+3
CG-20	II	---[c]	-28 (±5)	---
CG-21	II	-26 (±2)	-13 (±3)	-13
CG-32	V	-10 (±5)	-6 (±5)	-4
CG-34	V	-20 (±4)	-5 (±3)	-15
	Average	-18 (±4)	-15 (±4)	-7 (±7)

[a]Detailed data are given in the indicated report on this program

[b]Total dose 7×10^7 rads (H_2O)

[c]Electrolyte partially spilled

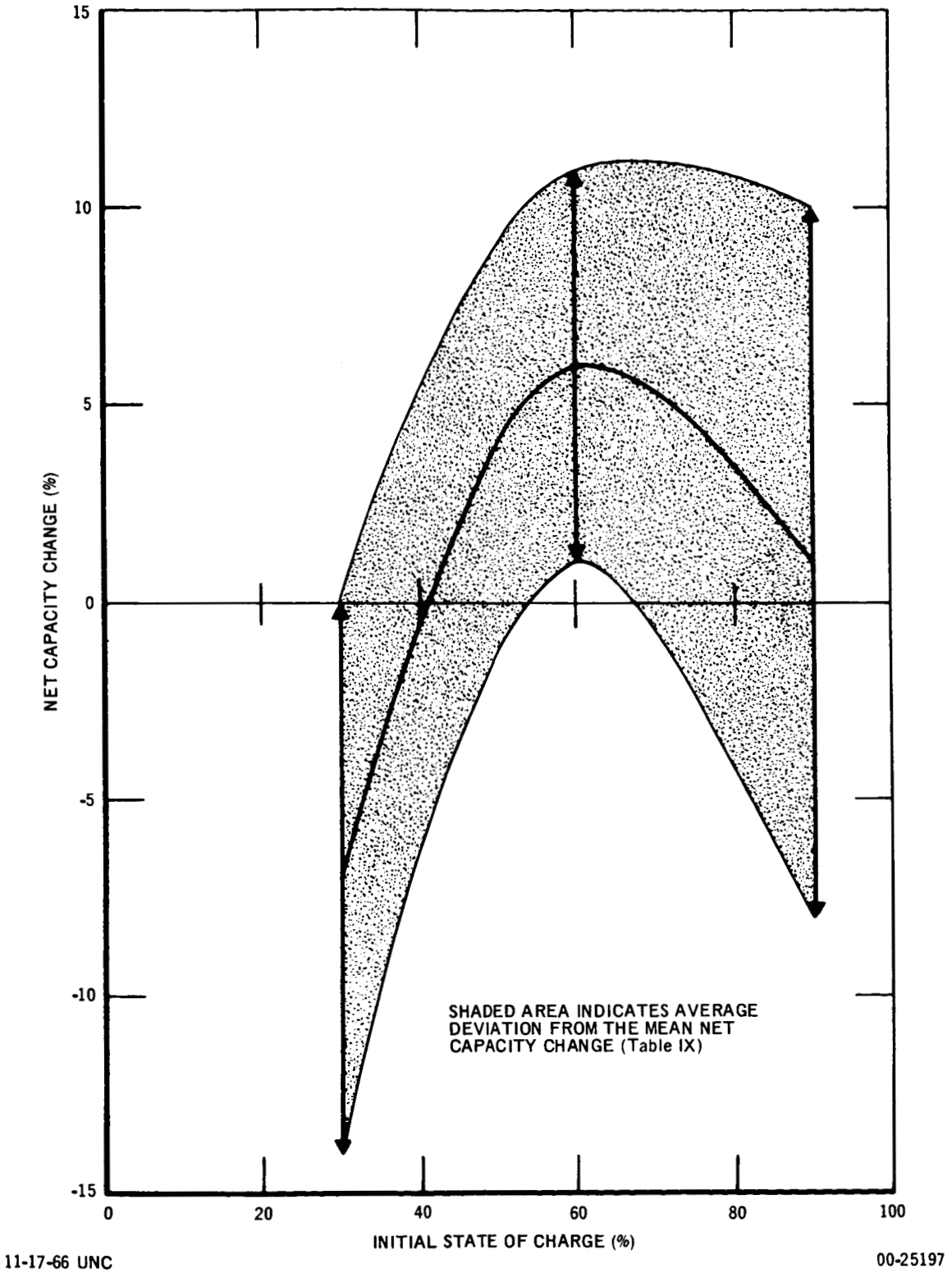

FIGURE 13. NET CHANGE IN SILVER ELECTRODE CAPACITY WITH RADIATION DOSE OF 7×10^7 RADS (H_2O)

due to temperature and/or cycling are larger in magnitude than the net changes associated with the irradiation process. Although the average changes are uncertain by several percent at each charge level, there appear to be a slight capacity decrease due to radiation at the 30% level, a comparable increase at 60% level, and essentially no change at 90%. Capacity changes over this charge range fall between average outer limits of +11% and -14%. A capacity gain may result from increased surface area. A loss of ~1.4% can be accounted for by the formation of residual solids in the cell. Since the relative proportion of AgO decreases with decreasing state of charge, some trends in the electrochemical response to radiation with the charge level would not be surprising. Characterization of the individual processes involved would require a more definitive scientific investigation beyond the scope of this program.

2. Hydrogen Evolution

The data on hydrogen evolution in experimental silver-cadmium cells are summarized in Table X, where final total pressures, percent hydrogen, and "G" values are given for irradiated cells at each charge level. Although substantial amounts of hydrogen were evolved in all runs, there is no trend in amount with the state of charge of the silver electrode. As mentioned in Section IVB, the gas evolution apparently occurs by the interaction of the active anode metal and hydroxyl radicals, which leaves an excess of radiolytically-produced hydrogen atoms to combine and form the gas. The state of charge of the silver electrode would then influence the gas evolution only through the related state of charge of the larger counter electrode. Table X pertains to silver-

TABLE X. HYDROGEN EVOLUTION IN SILVER-CADMIUM CELLS

Run	Initial State of Charge (%)	Radiation Dose (rads (H_2O))	Total Pressure (mm Hg)	Mole % H_2	G_{H_2}[a]
CG-16	90				
Irradiated Cell		7.2×10^7	1208	52.8	0.28
Control Cell		0	984	0.14	
CG-25	90				
Irradiated Cell		6.5×10^7	962	11.8	0.063
Control Cell		0	732	2.8	
CG-35	90				
Irradiated Cell		1.5×10^8	777	9.76	0.018
Control Cell		0	---[b]	---	
CG-36	90				
Irradiated Cell		9×10^8	928	39.1	0.013
Control Cell		0	760	0	
CG-17	60				
Irradiated Cell		7.2×10^7	988	15.1	0.058
Control Cell		0	971	0.10	
CG-26	60				
Irradiated Cell		6.5×10^7	1087	19.3	0.105
Control Cell		0	776	0.08	
CG-27	60				
Irradiated Cell		6.5×10^7	884	12.1	0.061
Control Cell		0	695	0	
CG-30	60				
Irradiated Cell		6.5×10^7	990	19.3	0.109
Control Cell		0	816	1.07	
CG-20	30				
Irradiated Cell		7.2×10^7	779	27.4	0.110
Control Cell		0	685	0.19	
CG-32	30				
Irradiated Cell		7.0×10^7	880	17.8	0.080
Control Cell		0	830	0.02	
CG-34	30				
Irradiated Cell		7.0×10^7	1120	15.3	0.067
Control Cell		0	892	0	

[a] Molecules H_2 per 100 ev absorbed by solution

[b] Faulty sampling

cadmium cells; further studies with zinc electrodes would be needed to evaluate the gas evolution characteristics more specifically for this metal in silver-zinc cells. By analogy to the cadmium cells, pressure increases of the order of 0.5 to 1 atm might be expected with doses of 10^8 rads and 50% ullage. Pressure containers or gas release valves may therefore be desirable for batteries in some space applications.

3. Material Loss

The losses of electrode material in the form of silver-containing residual solids recovered from both silver and cadmium compartments are shown in Table XI. The residual weights have been corrected for the content of silica dislodged from the fritted separators. The loss thus reported consisted primarily of silver, although silver oxides were detected occasionally by x-ray diffraction. The amounts of silver that migrated through the frits into the cadmium compartments were not significant when expressed as net changes on irradiation. Negative numbers in this column reflect the limits of experimental accuracy at the 1 to 2 mg/g level. Net losses in the silver compartments at a dose of 7×10^7 rads represent an average of 14 mg/g, or 1.4% of the total electrode weight in the uncharged condition. Some comments concerning the two high-dose runs were made in Section IV.A. This residual material would ordinarily be retained in a porous battery separator without serious damage to the cell. With excessive vibration, it might be channeled into sections that would tend to short the cell. However, a protective envelope such as cellophane, which is used to retard the growth of zinc dendrites, would also prevent shorting

TABLE XI. MATERIAL LOSS FROM THE SILVER ELECTRODE[a]

(A) Runs at 90% Initial State of Charge

Run	Milligrams of Residual Silver Solids per Gram of Silver Initially Present					
	Silver Electrode Compartment			Cadmium Electrode Compartments		
	Irradiated	Control	Net	Irradiated	Control	Net
CG-10	21.4	1.6	19.8			
CG-11	17.3	1.7	15.6			
CG-15	24.5	4.9	19.6			
CG-16	14.7	4.8	9.9			
CG-23	14.6	3.7	10.9			
CG-24	32	4.4	28	5.1	2.3	2.8
CG-25	39	5.6	33	2.1	3.9	-1.8
CG-35[b]	5.3	~1.2	4	0.9	1.6	-0.7
CG-36[c]	9.9	~2	8	2.5	1.2	-1.3

[a] 7×10^7 rads (H_2O) unless noted

[b] 1.5×10^8 rads

[c] 9×10^8 rads

TABLE XI. (Continued)

(B) Runs at 60% Initial State of Charge

Run	Milligrams of Residual Silver Solids per Gram of Silver Initially Present					
	Silver Electrode Compartment			Cadmium Electrode Compartments		
	Irradiated	Control	Net	Irradiated	Control	Net
CG-13	23.1	6.5	16.6			
CG-14	20.4	5.0	15.4			
CG-18	26.8	9.3	17.5			
CG-26	15.3	0.4	14.9	1.1	1.2	-0.1
CG-27	12.8	~0.3	12.5	4.0	1.4	2.6
CG-29	7.8	3.7	4.1	2.5	2.3	0.2
CG-30	~3	~2	~1	1.9	2.3	-0.9
CG-31	3.4	3.4	0	2.8	2.7	0.1

TABLE XI. (Continued)

(C) Runs at 30% Initial State of Charge

Run	Milligrams of Residual Silver Solids per Gram of Silver Initially Present					
	Silver Electrode Compartment			Cadmium Electrode Compartments		
	Irradiated	Control	Net	Irradiated	Control	Net
CG-19	50.2	22.1	28.1			
CG-20	52.6	--	--			
CG-32	6.2	2.1	4.1	2.7	2.4	0.3
CG-34	2.1	2.7	-0.6	1.6	0.8	0.8

by the silver residue. It is unlikely, therefore, that the silver losses associated with irradiation will present any new design problems for silver-zinc cells. For other silver batteries without retentive separators, a shorting problem might occur.

V. CONCLUSIONS AND RECOMMENDATIONS

Changes induced in silver electrode capacity by a radiation dose approaching 10^8 rads should not seriously affect battery performance in most applications. Average changes observed at this dose level were -7%, (±7%), +6% (±5%), and +1% (±9%) at 30, 60, and 90% states of charge, respectively. Although the study of zinc electrode behavior was less detailed, the capacity change observed or irradiation appeared to originate in the separator, rather than in the electrochemical system.

Provision should be made for radiation-induced pressure increases of the order of 0.5 to 1 atmosphere (assuming 50% ullage) in the design of silver-zinc or silver-cadmium batteries that may be exposed to as much as 10^8 rads. The evolved gas consisted of hydrogen and less-than-equivalent quantities of oxygen.

Material loss from the silver electrode was ~1.4% in flooded cells at the above dose level. Somewhat lower losses would be expected with closely-packed starved-electrolyte designs. Loss from the zinc electrode is expected to be primarily a function of separator characteristics.

If a more definitive characterization of individual radiation effects in the silver-zinc system is desired, a modified experimental approach is recommended. Such an approach would include the *in situ* application of fast electrochemical relaxation techniques to microelectrode systems in the radiation field. It would also include a larger proportion of diagnostic experiments on simplified porous

systems that would approximate battery electrode behavior without being subject to certain interactions that occur in complete battery systems.

ACKNOWLEDGMENTS

The experimental work on this program was performed by W. A. McCollum, R. E. Kelchner, and G. Schlesinger. N. M. Ewbank assisted project personnel in operation of the larger gamma radiation facility.

R. A. Holroyd of Atomics International was a consultant on radiation chemistry.

REFERENCES

1. Atomics International, "Radiation Effects on Nickel-Cadmium Battery Electrodes," AI-65-66, Final Report, Jet Propulsion Laboratory Contract 950514, June 1963 to April 1965
2. Atomics International, "Radiation Effects on Silver and Zinc Battery Electrodes," AI-65-158, Interim Report I, Jet Propulsion Laboratory Contract 951109, April 1965 to July 1965
3. Atomics International, "Radiation Effects on Silver and Zinc Battery Electrodes," AI-65-264, Interim Report II, Jet Propulsion Laboratory Contract 951109, July 1965 to October 1965
4. Atomics International, "Radiation Effects on Silver and Zinc Battery Electrodes," AI-66-33, Interim Report III, Jet Propulsion Laboratory Contract 951109, October 1965 to January 1966
5. Atomics International, "Radiation Effects on Silver and Zinc Battery Electrodes," AI-66-83, Interim Report IV, Jet Propulsion Laboratory Contract 951109, January 1966 to April 1966
6. Atomics International, "Radiation Effects on Silver and Zinc Battery Electrodes," AI-66-186, Interim Report V, Jet Propulsion Laboratory Contract 951109, April 1966 to July 1966